TISSUE ENGINEERING: Part A
Volume 18, Numbers 23 and 24, 2012

DOI: 10.1089/ten.tea.2012.0181

Engineered Contractile Skeletal Muscle Tissue on a Microgrooved Methacrylated Gelatin Substrate

Vahid Hosseini, Pharm.D., M.S.,[1,2,*] Samad Ahadian, Ph.D.,[1,*] Serge Ostrovidov, Ph.D.,[1] Gulden Camci-Unal, Ph.D.,[3,4] Song Chen, Ph.D.,[1] Hirokazu Kaji, Ph.D.,[5] Murugan Ramalingam, Ph.D.,[1,6] and Ali Khademhosseini, Ph.D.[1,3,4,7]

To engineer tissue-like structures, cells must organize themselves into three-dimensional (3D) networks that mimic the native tissue microarchitecture. Microfabricated hydrogel substrates provide a potentially useful platform for directing cells into biomimetic tissue architecture *in vitro*. Here, we present microgrooved methacrylated gelatin hydrogels as a suitable platform to build muscle-like fibrous structures in a facile and highly reproducible fashion. Microgrooved hydrogel substrates with two different ridge sizes (50 and 100 μm) were fabricated to assess the effect of the distance between engineered myofibers on the orientation of the bridging C2C12 myoblasts and the formation of the resulting multinucleated myotubes. It was shown that although the ridge size did not significantly affect the C2C12 myoblast alignment, the wider-ridged micropatterned hydrogels generated more myotubes that were not aligned to the groove direction as compared to those on the smaller-ridge micropatterns. We also demonstrated that electrical stimulation improved the myoblast alignment and increased the diameter of the resulting myotubes. By using the microstructured methacrylated gelatin substrates, we built free-standing 3D muscle sheets, which contracted when electrically stimulated. Given their robust contractility and biomimetic microarchitecture, engineered tissues may find use in tissue engineering, biological studies, high-throughput drug screening, and biorobotics.

Introduction

The ability to engineer human tissues *ex vivo* that could be used to replace diseased or damaged tissues *in vivo* is of great interest in biomedicine.[1] Such engineered tissues could also serve as tissue/organ models for drug discovery and biological studies.[2] Ideally, engineered tissues should have the same characteristics as the tissues that they were designed to mimic. For many tissues such as the myocardium,[3] smooth muscle,[4] and skeletal muscle,[5] the tissue function is closely linked to the cell organization and alignment. Therefore, controlling the structure and properties of the tissues by changing the extracellular matrix composition and substrate topography is crucial for proper cell alignment, organization, and differentiation.[6] In particular, skeletal muscle tissue is built from highly aligned myoblasts that fuse to form myotube-containing fibers, and this arrangement is vital for muscle contraction and functionality.[7]

Hydrogels have been used as three-dimensional (3D) tissue scaffolds due to their tissue-like mechanical properties and high oxygen and nutrient transport capacities.[8] The properties of hydrogels, including their ability to provide biological cues to cells, biodegradability, and solute transport, can be tuned. Consequently, hydrogels with various chemical and physical properties have been synthesized for regenerative medicine and tissue engineering applications.[9,10] In addition, recent developments in micropatterning and self-assembly have further enhanced the promise of hydrogels for tissue engineering and drug delivery.[11–14] Micropatterning approaches can be used to alter the behavior and fate of cells such as elongation,[15,16] differentiation,[17] and cell–cell contact and signaling.[18] Therefore, by combining micropatterning technologies and hydrogel microarchitecture, mechanical properties of scaffolds can be tuned to mimic those of the desired tissues.[19,20] In this work, we employed a gelatin methacrylate (GelMA) hydrogel as an underlying substrate to construct a functional muscle tissue.

[1]WPI-Advanced Institute for Materials Research, Tohoku University, Sendai, Japan.
[2]Department of Chemical and Biological Engineering, Chalmers University of Technology, Gothenberg, Sweden.
[3]Department of Medicine, Center for Biomedical Engineering, Brigham and Women's Hospital, Harvard Medical School, Cambridge, Massachusetts.
[4]Harvard-MIT Division of Health Sciences and Technology, Massachusetts Institute of Technology, Cambridge, Massachusetts.
[5]Department of Bioengineering and Robotics, Graduate School of Engineering, Tohoku University, Sendai, Japan.
[6]Institut National de la Santé Et de la Recherche Médicale U977, Faculté de Chirurgie Dentaire, Université de Strasbourg, Strasbourg, France.
[7]Wyss Institute for Biologically Inspired Engineering, Harvard University, Boston, Massachusetts.
*These two authors contributed equally to this work.

Skeletal muscle cells are highly sensitive to substrate stiffness, which influences their differentiation and contractibility.[21] When the substrate is stiff, for example, a conventional polystyrene culture dish or a glass slide, myotube contraction is isometric, but when the substrate is compliant such as a hydrogel substrate, contraction is isotonic.[22] Therefore, on the hydrogel substrate, the muscle remains at a constant tension while its length varies.

To date, most research has been focused on how to control the alignment and direction of muscle cells via the surface topography of the scaffold.[23–26] However, in these studies, the cell morphology and patterning were only controlled in 2D, and true 3D arrangements of cells have not yet been achieved. Other studies have used mechanical[27,28] or electrical stimulation[29] to align myotubes within hydrogels. For instance, myotube alignment was improved by mechanical stretching.[30] A few other methods, for example, cell-laden hydrogel patterning, have been successfully used to orient myoblasts in 3D.[31,32] Here, we present a simple and highly reproducible approach that directs murine C2C12 myoblasts into a 3D array by culturing the myoblasts on microgrooved GelMA hydrogels. By utilizing the microgrooves on GelMA hydrogels, we induced cellular alignment, elongation, and differentiation. In particular, two micropatterned hydrogels with ridges of different widths were employed to evaluate the role of ridge size on cellular behavior. To date, little work has been devoted to assess the effect of ridge size in micropatterned substrates on the cellular behavior. In addition, electrical stimulation was used to further induce myotube alignment and maturation of muscle fibers. Indeed, electrical stimulation has been shown to play the role of neural stimulation for an *in vitro* engineered muscle tissue.[33] Neurotization of engineered skeletal muscle significantly increases the contractile force that the tissue could generate.[34] We hypothesized that by integrating micropatterned hydrogels and electrical stimulation, it is possible to generate a harvestable 3D muscle tissue that had the ability to contract. The resulting engineered muscle tissues can be used in tissue engineering, fundamental biological studies, high-throughput drug screening, and micromuscle bioactuators.

Materials and Methods

Materials

The chemicals used in this study were gelatin Type A from porcine skin (Sigma-Aldrich), methacrylate anhydrate (Sigma-Aldrich), polydimethylsiloxane (PDMS, SILPOT 184; Dow Corning Toray Co. Ltd.), trimethoxysilyl propyl methacrylate (TMSPMA; Sigma-Aldrich), Dulbecco's modified Eagle's medium (DMEM; Invitrogen), fetal bovine serum (FBS; Bioserum), penicillin/streptomycin (P/S; Sigma-Aldrich), trypsin/EDTA (Invitrogen), minimum essential medium (MEM) essential amino acid solution (Invitrogen), Dulbecco's phosphate buffer saline (DPBS; Invitrogen), MEM nonessential amino acid solution (Invitrogen), and insulin (Invitrogen).

Cell culture

Murine C2C12 myoblast cells (less than six passages; American Type Culture Collection) were cultured under a 5% CO_2 atmosphere at 37°C in the DMEM, 10% (v/v) FBS, and 1% (v/v) P/S. When ~70% confluency was reached, the cells were detached by using 0.25% (w/v) trypsin/0.1% (w/v) EDTA and then subcultured or used in the experiment.

Preparation of the GelMA prepolymer

GelMA was synthesized as delineated in our previous work.[19] In brief, highly (~80%) methacrylated gelatin was produced by mixing 8 mL methacrylic anhydride with 10 g of type-A porcine-skin gelatin in 100 mL DPBS. The mixture was stirred at 50°C for 3 h. The reaction was stopped by diluting the mixture fourfold with warm (40°C) DBPS. The mixture, in a 12–14-kDa cutoff dialysis tube, was dialyzed against distilled water for 1 week at 40°C and then lyophilized. A mixture of 20% (w/v) GelMA and 1% (w/v) photoinitiator [i.e., 2-hydroxy-1-(4-(hydroxyethoxy) phenyl)-2-methyl-1-propanone or Irgacure 2959] (CIBA Chemicals) in DPBS was kept at 70°C until GelMA fully dissolved. The GelMA prepolymer was used to make micropatterned GelMA hydrogels in the experiments.

PDMS stamp preparation

A silicon wafer patterned with an SU-8 photoresist pattern was made using the conventional photolithography method.[35] This template was then used to make PDMS stamps as follows. PDMS prepolymer and its curing agent were mixed at 10:1 ratio (w/w) and poured onto the silicon master mold, and the mold was held under vacuum for 15 min to remove air bubbles. The master mold/PDMS system was then spun at 300 rpm to reduce the PDMS thickness to a few millimeters. After the system was cured at 70°C for 2 h, PDMS stamps were peeled off the master mold and then silanized with trichloro(1H, 1H, 2H, 2H-tridecafluro–n–octyl) silane (Tokyo Chemical Industry Co.) to prevent adhesion of the GelMA hydrogels to the stamp.

Micromolding of GelMA hydrogels and cell seeding

GelMA hydrogels were molded on the surfaces of standard cell culture plates (Orange Scientific) or glass slides. Briefly, 15 μL of the GelMA prepolymer (sufficient to cover a 10×10 mm area) was poured on a Petri dish or a glass slide, and a PDMS stamp was placed into the prepolymer. The stamp was softly rubbed so that its microgrooves were filled with the prepolymer, and then the stamp and prepolymer were exposed to 7 mW/cm^2 UV light (Hayashi UL-410UV-1; Hayashi Electronic Shenzen Co., Ltd) for 150 s. The stamp was then gently removed to obtain a micropatterned GelMA hydrogel. Two types of micropatterned hydrogels were prepared: one with a 100-μm groove–50-μm ridge pattern and the other with a 100-μm groove–100-μm ridge pattern (hereafter, we denote them as narrow- and wide-ridge micropatterns, respectively).

To build a free-standing patterned hydrogel sheet, one-fourth of a glass coverslip was coated with TMSPMA, so that the GelMA prepolymer can easily be adhered to this portion of the glass. To do so, the glass coverslip was partially immersed in 1% (v/v) TMSPMA/methanol for 30 min followed by oven-drying at 100°C for 1 h (Supplementary Fig. S1; Supplementary Data are available online at www.liebertpub.com/tea).

To culture the cells on the hydrogels (Fig. 1), the cells were first trypsinized, counted, and then resuspended in the

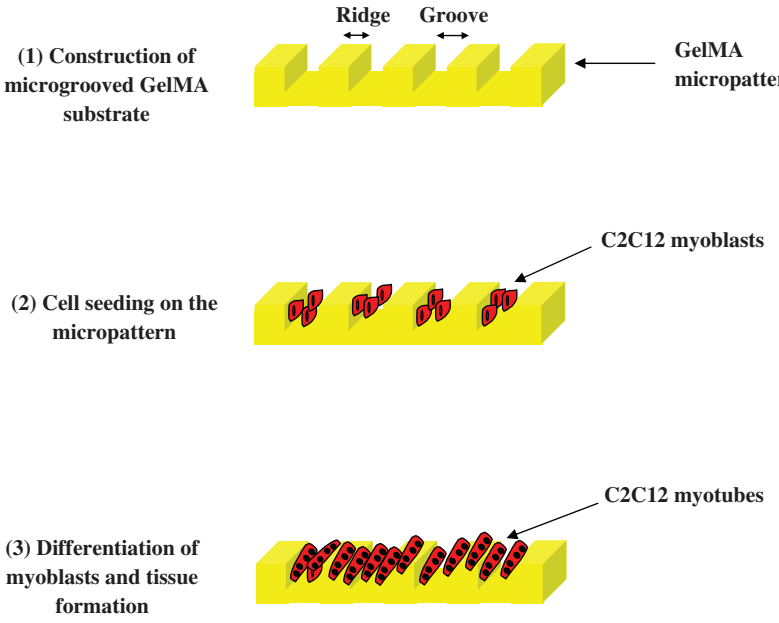

FIG. 1. Schematic procedure to engineer myofibers on microgrooved gelatin methacrylate (GelMA) substrates. Color images available online at www.liebertpub.com/tea

DMEM at a density of 2×10^6 cells/mL. Following the protocol of Nelson and colleagues,[36] 100 µL of the cell suspension was placed onto a micropatterned hydrogel, in the Petri dish, and then the system was left undisturbed for 15 min at 37°C to allow the C2C12 myoblasts to attach to the insides of the grooves. The culture medium was then added to the dish and immediately aspirated to remove nonadherent cells. A fresh medium was then added, and the cells were cultured for 1 day, at which point the cell layers inside the microchannels were nearly confluent. The medium was then replaced with a differentiation medium (DMEM, 2% [v/v] horse serum [Invitrogen], 1 nM insulin [Invitrogen], 1% [v/v] P/S), and the culture was continued for 2 weeks. The medium was normally changed every 2 days.

Quantification of myoblast alignment

After 3 days of culture on the hydrogel substrates, myoblasts were fixed by using 4% (w/v) paraformaldehyde for 12 min, permeabilized with 0.3% (v/v) Triton X-100 for 10 min, blocked by using 5% (w/v) bovine serum albumin for 20 min, and then stained with phalloidin (Alexa-Fluor 594; Invitrogen) and 4′,6-diamidino-2-phenylindole dihydrochloride (DAPI; Sigma-Aldrich) as recommended by the manufacturer's instructions to reveal filamentous F-actin and cell nuclei, respectively. The cells were imaged with a fluorescence microscope (Carl Zeiss Observer Z.1). Alignment of DAPI-stained cell nuclei was quantified as described earlier.[16] The alignment angle, defined as the orientation of the elliptic axis of a nucleus to the elliptical horizontal axis, was calculated for more than 200 nuclei in each experiment using the ImageJ software package. The normalized alignment angles with respect to the preferred orientation were defined as the mean orientation of all nuclei in a sample. Alignment angles were then categorized in 10° increments to the preferred orientation. Cells that were aligned within 10° of the preferred orientation were counted as the aligned cells.[32]

Quantification of myotube alignment and morphological characterizations by immunostaining

Cells were fixed and permeabilized as described above. The samples were covered with the mouse monoclonal antifast skeletal myosin antibody (1:1000 dilution, ab-7784; Abcam) in DPBS, which were then kept at 4°C for 24 h. Samples were then treated with Alexa-Fluor-488-conjugated goat anti-mouse antibody (1:1000 dilution; Invitrogen) in DPBS and incubated for 1 h at 37°C. To visualize α-actinin, the samples were incubated with monoclonal anti-α-actinin antibody (1:1000 dilution, EA 53; Sigma-Aldrich) in DPBS for 1 h at ambient temperature and then treated with Alexa-Fluor-594-conjugated donkey anti-mouse IgG (Invitrogen) for 1 h. Fluorescence micrographs at different magnifications were acquired to visualize the myotubes. Images were acquired at days 3, 6, 8, and 14 of cell culture, and then images of at least 50 myotubes were analyzed. Here, myotubes were defined as multinucleated muscle myofibers having at least three cell nuclei. Myotube lengths, widths, and orientation angles were measured with AxioVision Rel. 4.8, and their relative surface area coverage was quantified with the NIH ImageJ software package. The aspect ratio for each myotube was calculated by dividing the myotube length by its widest width.[37]

Electrical stimulation of myotubes

The arrangement of the electrodes used to electrically stimulate the myotubes is shown in Supplementary Figure S2. The electrodes were 0.6-mm-diameter platinum wires, and the separation between them was 3.5 cm. The differentiation medium was the DMEM culture medium supplemented with 2% horse serum, 1 nM insulin, 2% MEM essential amino acid solution, 1% MEM nonessential amino acid solution, and 1% P/S.[38] Electrical pulse stimulation (amplitude 22 mA, frequency 1 Hz, and duration 2 ms) was applied to the samples via the electrodes that were connected to an electronic stimulator (SEN-8203; Nihon Kohden) equipped with an isolator unit (SS-104J; Nihon Kohden).

Electrical stimulation of myotubes began at day 6 of culture and continued for the next 48 h. Tissue or myotube contraction was assessed at 1 and 2 days after the start of the stimulation. When recording the movies that show tissue or myotube contraction, the pulse duration was changed to 102 ms.

Statistical analysis

The independent Student's *t*-test was used to compare two data sets by the MINITAB statistical software package version 13.0, Minitab, Inc. The results were reported as the mean ± standard deviation. Calculated p-values < 0.05 were considered significant.

Results and Discussion

C2C12 myoblast and myotube alignment

Cells respond to physical signals in their surroundings such as surface topography and substrate stiffness.[39,40] In our experiments, the C2C12 myoblasts that were cultured on the micropatterned GelMA hydrogels were significantly more aligned at day 3 of culture than the control cells that were cultured on nonpatterned hydrogels (Fig. 2). However, no significant difference between the cell alignments for the two GelMA micropatterns was found. Nuclear alignment was also quantified along the 40-μm depth of the grooves to assess cell alignment in the vertical dimension. The results indicated that the micropatterned myoblasts aligned in layers throughout the 3D structure of the tissue fiber (Fig. 3).

After inducing differentiation, the C2C12 myoblasts fused together and formed multinucleated C2C12 myotubes. It is noteworthy that cells appeared to differentiate onto the ridge surfaces in addition to GelMA microgrooves. Therefore, homogeneously organized muscle fibers were obtained for both micropatterns as demonstrated in Figure 4; however, the difference in the abilities of the two micropatterns to align the myotubes onto the groove and ridge surfaces was visible as demonstrated in Figure 5, where the myotubes were less guided by the created topography on the GelMA hydrogel

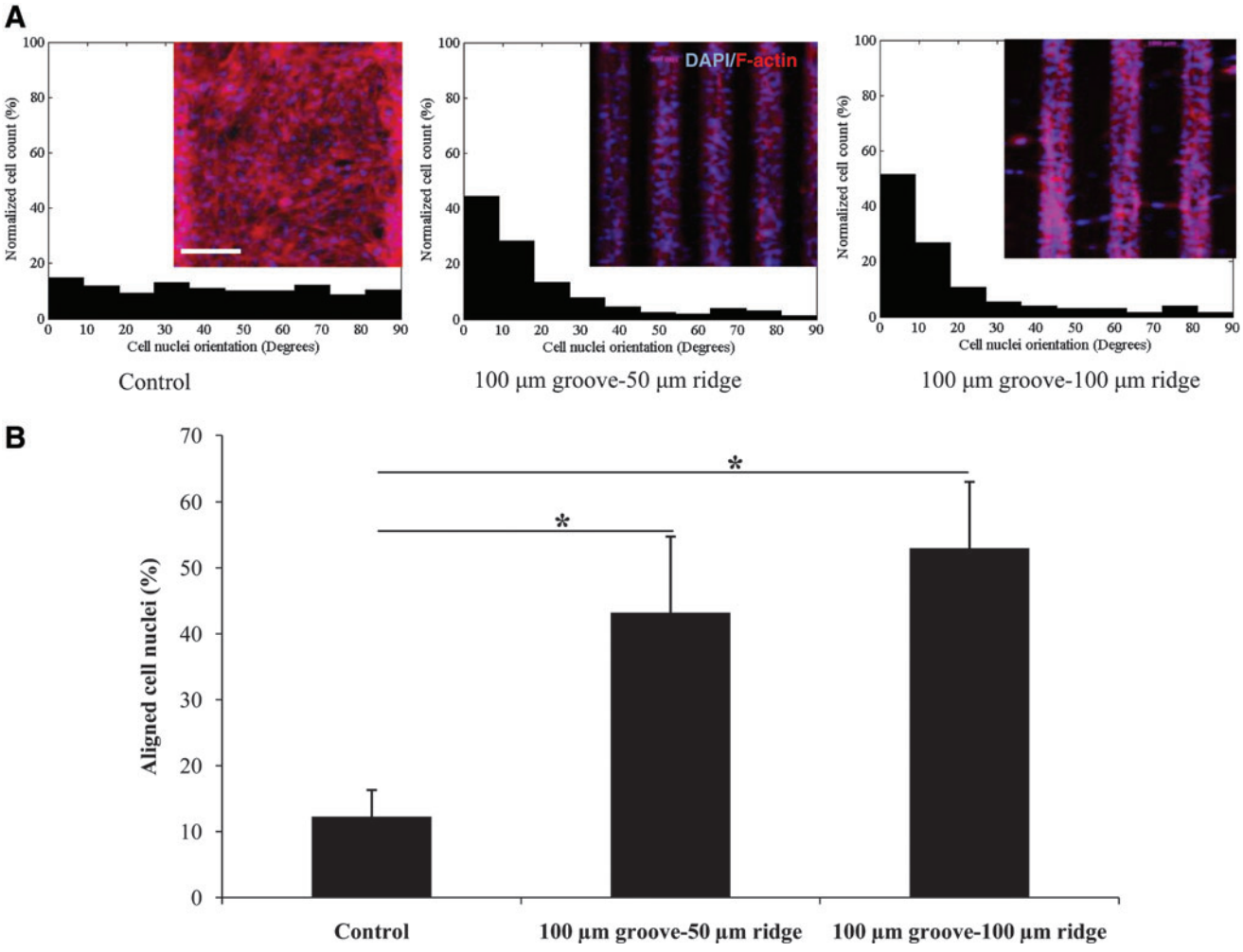

FIG. 2. Alignment of cells on microgrooved and flat GelMA substrates after 3 days in culture. **(A)** Histograms showing the relative cell numbers as a function of their relative alignments (in 10° increments). The micropatterns increased the degree of cellular alignment in comparison to that of the nonpatterned substrates (control). Inserts show representative images of 4′,6-diamidino-2-phenylindole dihydrochloride (DAPI)/F-actin-stained cells. **(B)** Percentage of cells aligned within 10° of the orientation of the grooves for various substrates. The C2C12 myoblasts in narrow- and wide-ridge micropatterns were significantly more aligned than those in the flat GelMA substrate (scale bar, 150 μm; $*p < 0.001$). Color images available online at www.liebertpub.com/tea

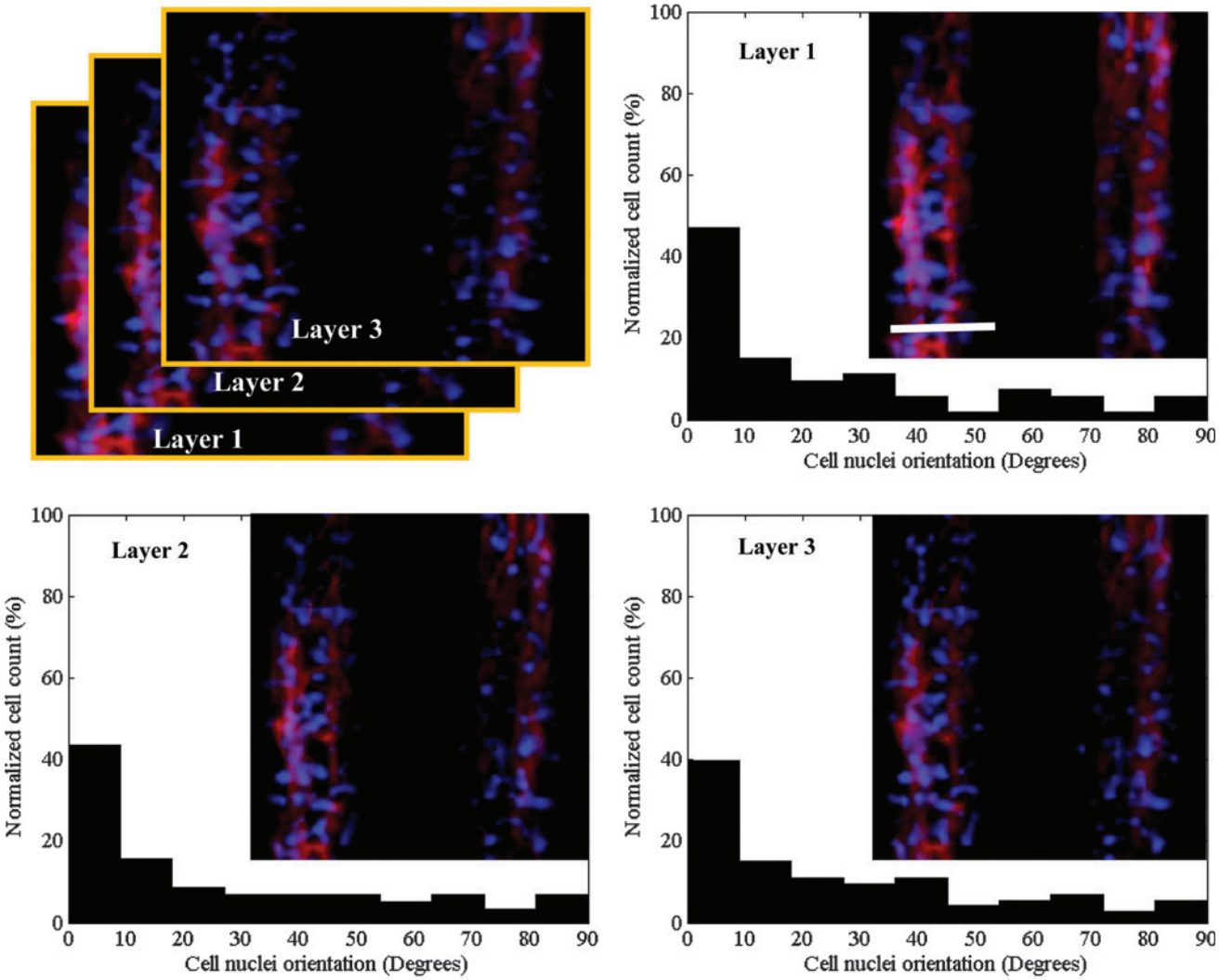

FIG. 3. Alignment of cells within the channels of the 100-μm groove–100-μm ridge micropatterned GelMA hydrogels after 3 days in culture. Histograms show the percentage of cells visualized as 10-μm-thick layers along the *z*-axis that have alignments (in multiples of 10°) relative to the preferred alignments. Inserts: representative images of DAPI/F-actin-stained cells (scale bar, 100 μm). Color images available online at www.liebertpub.com/tea

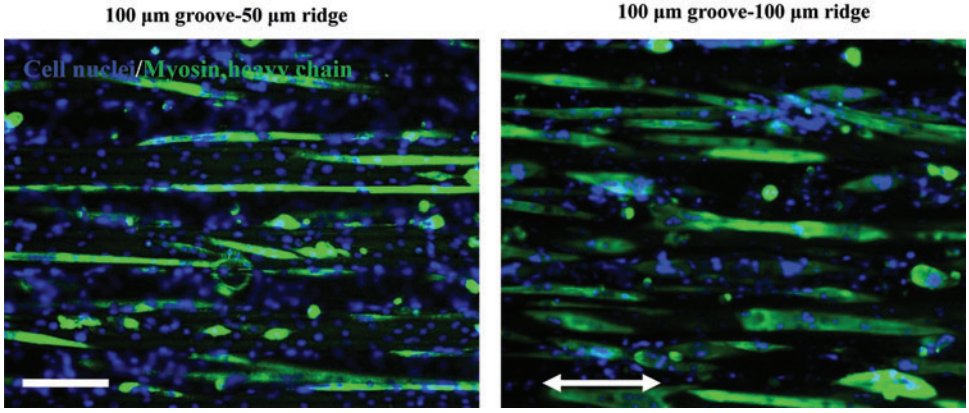

FIG. 4. C2C12 myotubes within underlying microgrooved GelMA hydrogels, namely 100-μm groove–50-μm ridge and 100-μm groove–100-μm ridge micropatterns at day 6 of culture. Note that the aligned C2C12 myotubes formed homogeneously organized muscle tissues. The length of the double-headed white arrow is aligned parallel to the microgroove direction (scale bar, 50 μm). Color images available online at www.liebertpub.com/tea

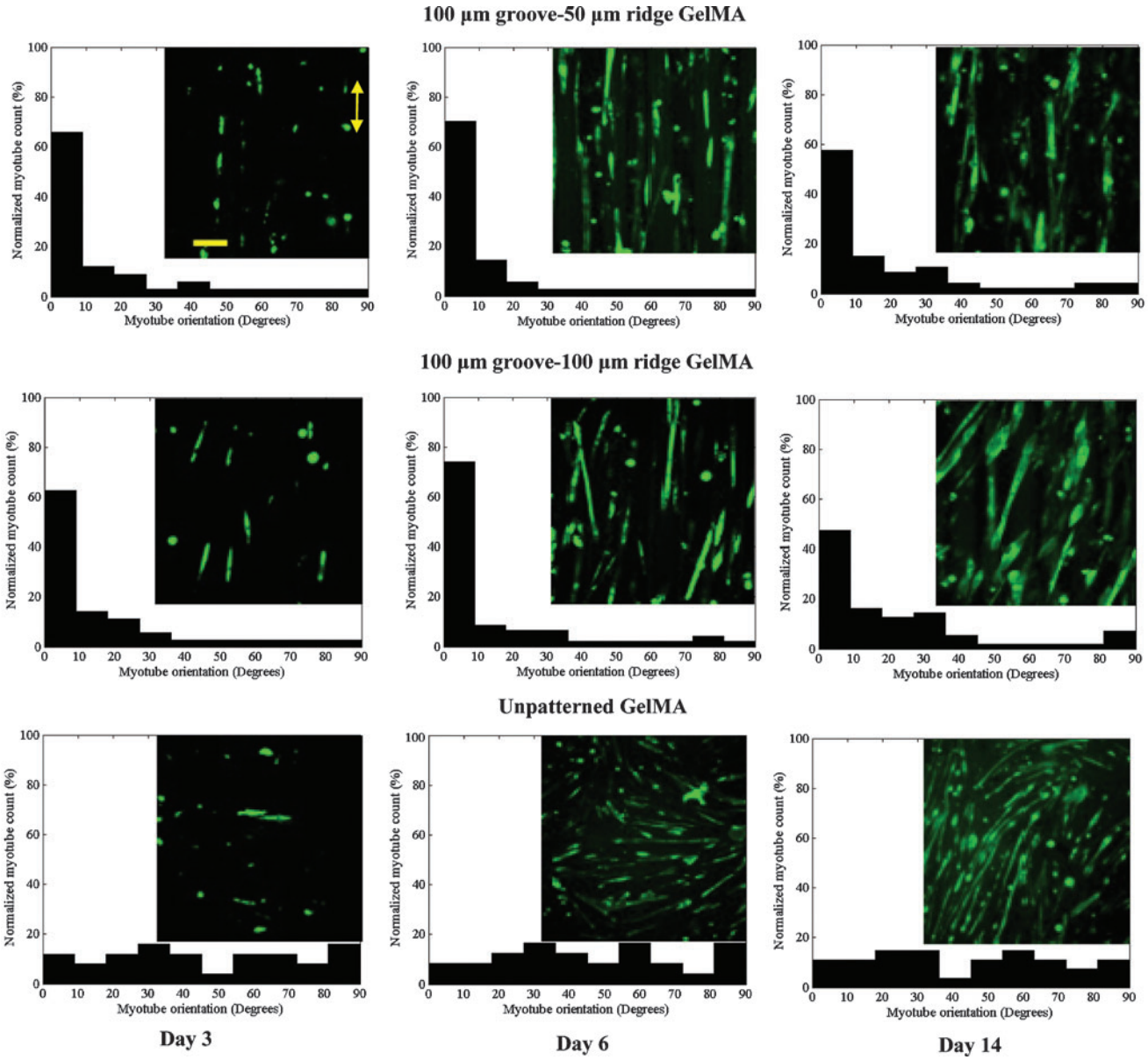

FIG. 5. Alignment of myotubes at days 3, 6, and 14 of culture for the unpatterned and micropatterned GelMA hydrogels. Histograms show the percentage of myotubes that were aligned (in multiples of 10°) relative to the preferred alignments (i.e., direction of the grooves). The micropatterned myotubes were highly aligned compared with the unpatterned myotubes. Inserts: representative images of anti-myosin heavy-chain-stained myotubes. The length of the double-headed yellow arrow is aligned parallel to the microgroove direction (scale bar, 100 µm). Color images available online at www.liebertpub.com/tea

with 100-µm ridge than that with 50-µm ridge. This observation is in accordance with previous studies in which the myotubes were less aligned in the wide-ridge systems.[33,34] Indeed, highly organized myotubes are essential to fabricate a functional muscle tissue and in particular for the function of load-bearing muscles.[41] Therefore, finding a suitable biomaterial that can help individual myoblasts organize into a functional muscle is of importance. *In vitro*, cells have been manipulated to modify their microenvironment and organize over short distances, but rarely they can be induced to form long-range anisotropic structures, which are needed to make functional tissues.[42] GelMA hydrogels are promising materials for tissue engineering applications, because cells cultured on them can migrate, proliferate, and contact with each other, which may be used to create 3D networks that mimic functional tissues *in vitro*.[32] The mechanical properties of GelMA hydrogels are tunable, and the high diffusion capacity created by the hydrogel pores is advantageous for cell nutrition and waste removal.[20]

By the second week of culture, the myotubes were more aligned on the micropatterned hydrogels than the myotubes on the unpatterned hydrogels ($p < 0.001$; Fig. 5), which coincides with the result of a previous study.[43] At day 6 of culture, the maximum alignment, which involved >70% of the myotubes, for both micropatterned systems were achieved. Thereafter, the percentages of aligned myotubes slightly decreased. More precisely, myotube alignment was decreased at day 8 of culture for the wide-ridge micropattern

system and at day 14 of culture for the narrow-ridge micropattern system. This alignment reduction might have been caused by increases in the thickness of the myotube layers and formation of new myotubes, which were less affected by the micropattern topographies. Indeed, fluorescence micrographs revealed that the myotubes, especially those in the upper layers, were not oriented in the microgrooved direction. By decreasing the ridge width from 100 to 50 μm, a significant ($p < 0.05$) improvement in myotube alignment was observed. Therefore, the ridge width greatly influenced myotube orientation.

Myotube morphology

We found that the surface area covered by the myotubes dramatically increased between days 3 and 6 of culture and then remained almost unchanged (Fig. 6A). It seems that

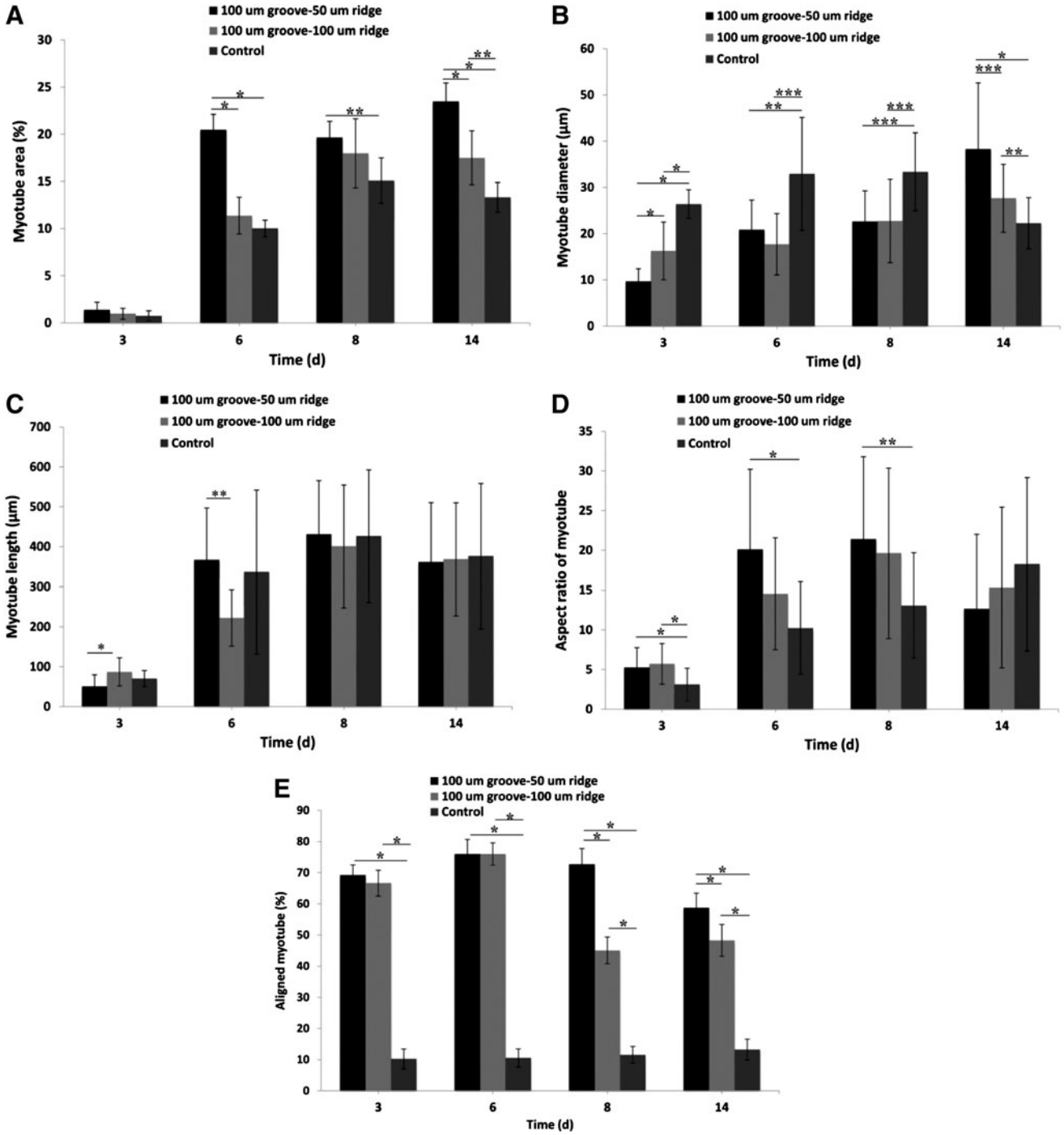

FIG. 6. Morphological properties of the muscle-like structures in the microgrooved and smooth GelMA substrates. **(A)** Area, **(B)** diameter, **(C)** length, **(D)** aspect ratio, and **(E)** alignment measured on days 3, 6, 8, and 14 of culture. The myotubes in the 100-μm groove–50-μm ridge and 100-μm groove–100-μm ridge micropatterned hydrogels are of a better quality than those in the unpatterned substrates (*$p < 0.001$; **$p < 0.01$; and ***$p < 0.05$).

during the first 6 days of culture, the fusion of C2C12 myoblasts into myotubes was mostly occurred. Interestingly, the area covered by myotubes was significantly greater ($p < 0.05$) for the narrow-ridge micropattern than that for the wide-ridge micropattern, which indicated a larger fusion rate induced by the narrower surface. This justification can be made as both surfaces were fully covered by cells at this time point. In addition, the difference in the myotube coverage areas of the narrow-ridge GelMA micropattern and unpatterned GelMA substrate was significant at day 6 of culture and remained significant thereafter, whereas the difference between the wide ridge GelMA micropattern and flat GelMA substrate was significant only at day 14 of culture (Fig. 6A). Therefore, the reduction in the ridge width in a ridge–groove micropattern may have increased the rate of C2C12 myoblast differentiation.

The mean diameter of the myotubes in the unpatterned system was larger than that of the myotubes in both micropatterned systems until day 8 of culture (Fig. 6B), probably because it was initially easier for the control myoblasts to fuse laterally. Clark *et al.* also found similar differences in myotube diameters where a parallel micropatterned silicon wafer was used to align myotubes.[24] By day 14 of culture, the mean diameters of the myotubes in both micropatterned systems were larger than that of the control, and the increase was especially significant for the narrow-ridge micropatterned samples ($p < 0.01$).

The myotube length increased until day 6 of culture and then remained constant (Fig. 6C), with the mean myotube length in the narrow-ridge micropattern significantly larger than that in the wide-ridge micropattern ($p < 0.05$). Therefore, the narrow-ridge micropattern improved the end-to-end contact and fusion rate. This may be because the degree of alignment for the myotubes on the narrow-ridge micropattern was higher than that for the wide-ridge micropattern. Therefore, there is a higher probability of end-to-end contacts for the narrow-ridge micropatterns as compared to the wide-ridge micropatterns. Consequently, the aspect ratio was sharply increased from day 3 of culture as a result of increases in myotube lengths and remained constant after day 6 of culture. Significant differences in myotubes lengths among the micropatterned and unpatterned samples were not found at days 8 and 14 of culture.

In general, the narrow-ridge GelMA micropattern had a more significant impact on the cell behavior than the wide-ridge GelMA micropattern, in particular on myotube properties in terms of diameter, coverage area, aspect ratio, and alignment, which suggests that the narrow-ridge GelMA micropatterns may have provided a more suitable microenvironment for the construction a functional muscle tissue compared to the wide-ridge GelMA micropatterns.

Electrical stimulation of myotubes

Electrical stimulation has been used to induce differentiation of myoblasts aligned in 2D and 3D arrays.[13,29,43,44] For example, Flaibani *et al.* studied the effect of long-term electrical stimulation on myoblasts cultured on a 50-μm groove–50-μm ridge micropatterned polylactic acid and found a greater rate of myoblast differentiation compared to the control system; however, no significant changes in myotube alignment was observed.[29] In this work, for the electrically stimulated myotubes in the wide-ridge micropatterns, the coverage area significantly increased when compared with those in the nonpatterned samples ($p < 0.05$, Fig. 7A). Other researchers have found that electrical stimulation enhanced myotube formation and increased the myoblast differentiation rate[29,45] where long-time electrical stimulation regimes were employed and begun on the first day of culture. However, our electrical stimulation regime did not influence the myoblast differentiation rate probably because the greatest degree of myotube formation was already obtained before electrical stimulation was applied.

Interestingly, electrical stimulation further aligned the myotubes in the micropatterned systems, especially those in the wide-ridge GelMA micropatterns (Figs. 7E and 8). To better visualize the myotubes aligning during electrical stimulation, we filmed the myotubes in the wide-ridge micropattern during the first 7 h of electrical stimulation (Supplementary Movie S1), which shows that the slanted myotubes from the preferred orientation detach, reorganize, and consequently improve the total myotube alignment. Apparently, the stiffness of the GelMA hydrogel, which is close to that of native muscle tissue (~ 12 kPa[22]), promoted myotube isotonic contraction as the cells sensed an *in vivo*-like environment. Indeed, only nonrigid biomaterials, such as GelMA hydrogels, can induce isotonic muscle contractility. The suitable flexibility of the GelMA hydrogel allowed the myotubes to gradually reorganize without detaching from the substrate, which commonly occurs when myotubes on a rigid material, for example, PDMS or glass, are electrically stimulated.[38] The improvement in the myotube alignment in the narrow-ridge micropattern was less than that in the wide-ridge micropattern. It was reported that electrical stimulation (ES) had a significant effect on the alignment of primary cardiomyocytes and human adipose-derived stem cells.[46] For example, Tandon *et al.*[47] compared the effects of ES and topographical cues on cardiac cell alignment and elongation. They observed that application of an electrical field either parallel or orthogonal to the direction of the cells did not change the direction or elongation of the cells. Therefore, they concluded that the alignment and elongation pathway was saturated by the topographical cue, and that the same signaling pathways control the cellular response to electrical and topographical cues. Similarly, the same trend was reported by Au *et al.*[48,49] in which cardiomyocytes were cultured on a chip to simultaneously evaluate the effects of electrical and topographical cues. In the previous studies, stiff substrates were used, whereas in our study, we used a soft substrate. Thus, it appears that the differences in our observations may be due to the effects of substrate stiffness. As recently demonstrated by Bhana *et al.*,[50] cardiac cells cultured on substrates with a stiffness comparable to that of the native cardiac tissue exhibited optimal cell morphology and function.

Electrical stimulation also significantly increased the diameters of the myotubes in both micropatterned systems ($p < 0.05$, Fig. 7B). When not electrically stimulated, the unpatterned myotubes had a greater diameter on average than did the micropatterned myotubes. When electrically stimulated, the diameters of the micropatterned myotubes increased significantly until they were the same size, on average, as the stimulated unpatterned myotubes (Fig. 7B). The mean diameter of myotubes in the narrow-ridge micropatterns significantly improved in comparison with that

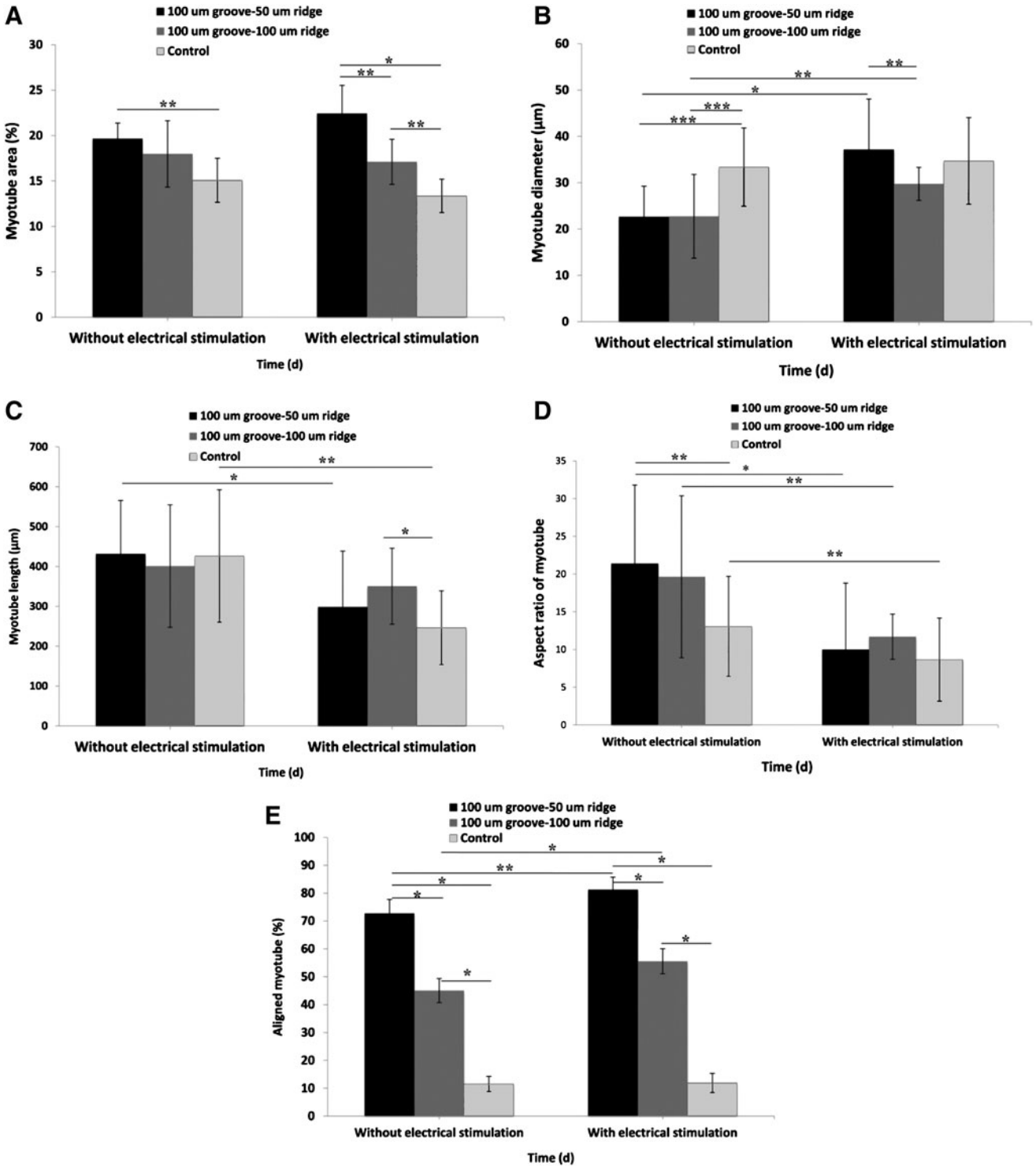

FIG. 7. Effect of the 2-day electrical stimulation on myotube **(A)** area, **(B)** diameter, **(C)** length, **(D)** aspect ratio, and **(E)** alignment (*$p < 0.05$; **$p < 0.01$; and ***$p < 0.001$).

in the wide-ridge micropatterns ($p < 0.05$). Myotube lengths decreased in all samples after 2 days of electrical stimulation (Fig. 7C), as did the aspect ratios, probably as a result of myotube shortening (Fig. 7D). When myotube morphologies were compared at day 8 of culture, we observed that both myotube lengths and diameters were enhanced by electrical stimulation for wide-ridge micropatterns, whereas only the myotube diameters increased for the narrow-ridge micropatterns as compared with the nonstimulated samples. Given the aforementioned observations, we conclude that electrical stimulation globally improved the myotube quality. This conclusion is supported by the work of Liao and coworkers, who observed that the contractile proteins myosin and α-actinin were upregulated by electrical stimulation.[51] Increases

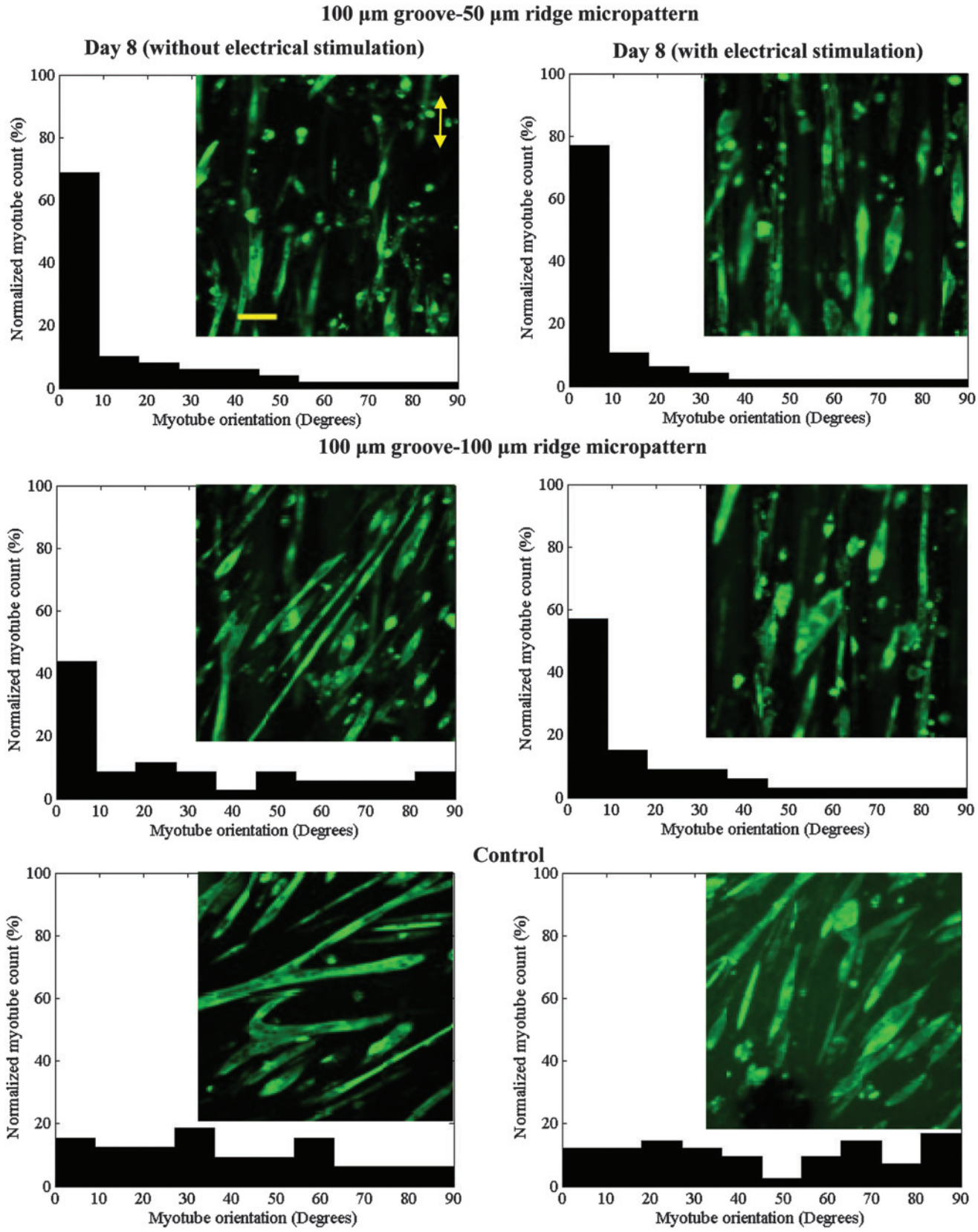

FIG. 8. Effect of electrical stimulation on the alignments of myotubes cultured on micropatterned and unpatterned GelMA hydrogels. The histograms show the relative numbers of myotubes that had alignments (in multiples of 10°) relative to the preferred alignments. The alignments of the myotubes in the micropatterned systems improved with electrical stimulation. Inserts: representative images of anti-myosin heavy-chain-stained myotubes. The direction of microgrooves is parallel to the double-headed yellow arrow (scale bar, 100 μm). Color images available online at www.liebertpub.com/tea

in the myotube diameter have also been found in native muscles after doing a physical exercise.[52] Immunofluorescence images (Fig. 9) showed that Z-lines were clearly formed in electrically stimulated samples compared to the nonstimulated ones, indicating that the myosin and α-actin in contractile proteins were highly expressed in the electrically stimulated muscle tissues.

The contraction of the engineered tissues was recorded 1 and 2 days after starting electrical stimulation. The myotube displacements due to the electrical stimulation were increased in all samples during the course of the electrical stimulation (Supplementary Movies S2–S4). Therefore, the current electrical stimulation regime improved the contractile ability of the myotubes.

Construction of the free-standing 3D muscle tissue

To show that muscle tissue grown on the GelMA hydrogel could be harvested, we created the free-standing 3D muscle tissue having contractile ability. The portions of this construct that were not permanently attached to the glass slides (Supplementary Fig. S1) were easy to handle, suggesting that such a system could be used in micromechanical devices such as biorobots or bioactuators. Supplementary Movie S5

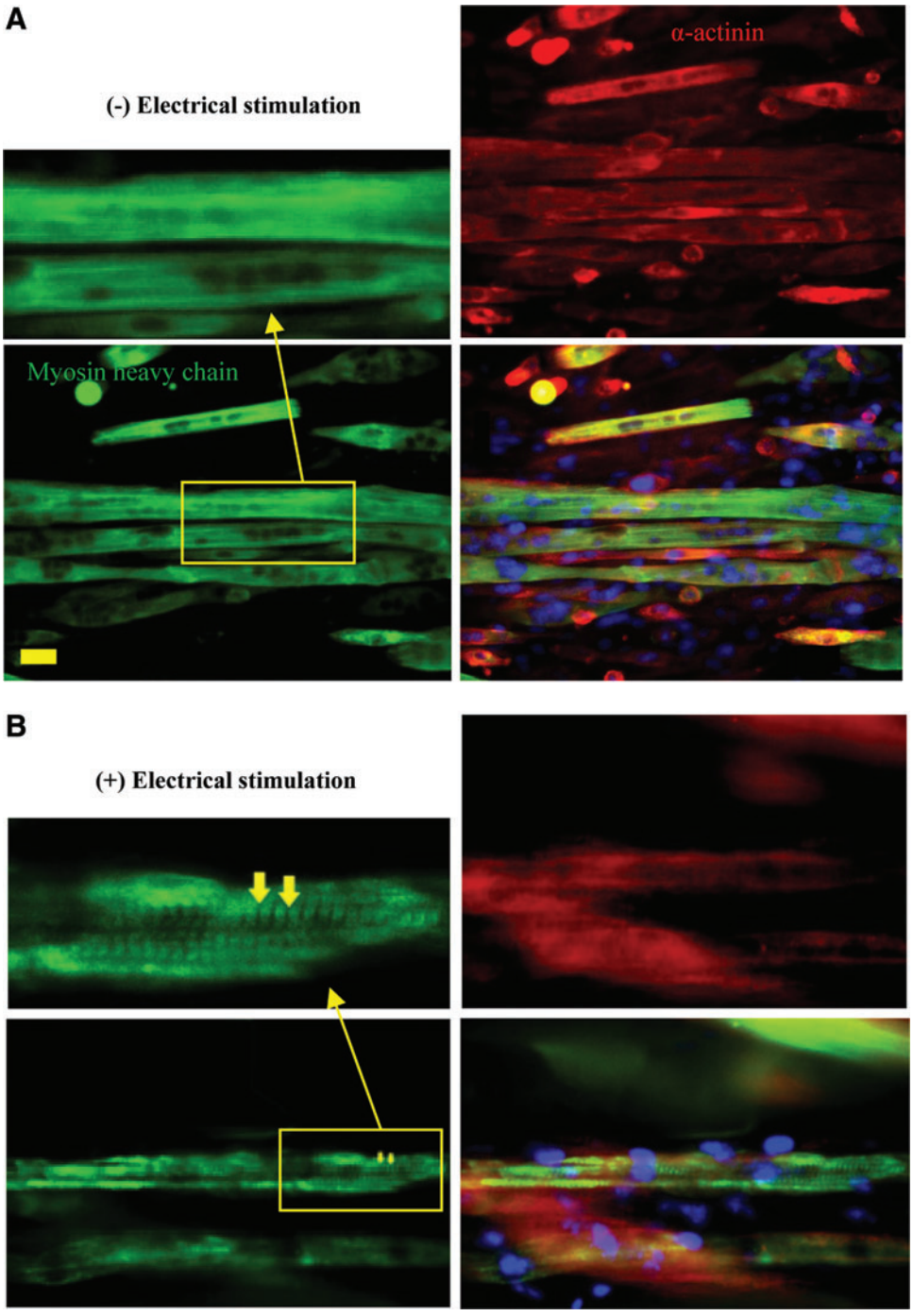

FIG. 9. Immunofluorescence micrographs of myosin heavy chains (green), α-actinin (red), and nuclei (blue) for myotubes cultured on the wide-ridge GelMA hydrogel at day 8 of culture without **(A)** or with **(B)** electrical stimulation. Arrows identify myotube Z-line striation (scale bar, 50 μm). Color images available online at www.liebertpub.com/tea

shows the middle portion of the free-standing tissue contracting after 1 day of electrical stimulation. Supplementary Movie S6 shows the same muscle tissue contracting when viewed along its side. To the best of our knowledge, this is the first attempt to construct a muscle tissue that can contract when electrically stimulated on a biodegradable GelMA hydrogel. Previously, many attempts at creating 3D contractile muscle tissues were made on a natural material, such as, collagen or fibrin, or were assembled on an anchored muscle sheet.[13,16,23] The properties of natural materials promote cell proliferation and differentiation. However, they are mechanically weak, which makes it hard to control the properties of the final tissue construct, for example, geometry, elasticity, stiffness, and biodegradability. In this regard, GelMA hydrogels may be an appropriate scaffold for muscle tissue engineering applications, high-throughput drug screening, and designing the next generation of micromuscle actuators.

Conclusions

In summary, we introduced microgrooved GelMA hydrogels as a suitable platform to build muscle-like fibrous structures in a facile and highly reproducible manner. Microgrooved hydrogel substrates with two different ridge sizes (50 and 100 μm) were fabricated to evaluate the effect of the distance between engineered myofibers on the orientation of the bridging C2C12 myoblasts and the formation of the resulting C2C12 myotubes. It was demonstrated that although the ridge size did not significantly affect the C2C12 myoblast alignment, the wider-ridged micropatterned hydrogels generated more myotubes that were not aligned to the groove direction than those on the smaller-ridge micropatterns. We also demonstrated that electrical stimulation improved the myoblast alignment and increased the diameter of the resulting myotubes. Free-standing 3D muscle sheets having contractile ability upon applying the electrical stimulation were also fabricated. It is expected that the engineered tissues may find use in tissue engineering, biological studies, high-throughput drug screening, and micromuscle actuators due to their robust contractility and biomimetic microarchitectures.

Acknowledgments

V.H. and S.A. conceived the idea and designed the research. V.H., S.A., H.K., M.R., and A.K. analyzed the results. V.H. and S.A. contributed equally to the work and wrote the article. V.H., S.A., S.O., and G.C-U. performed the experiments. H.K., A.K., and M.R. supervised the research. All authors read the manuscript and approved its content. This work was supported by World Premier International Research Center Initiative, MEXT, Japan, and a Grant-in-Aid for Young Scientists (A) (23681027) to H.K. from the Ministry of Education, Science, and Culture, Japan.

Disclosure Statement

No competing financial interests exist.

References

1. Khademhosseini, A., Vacanti, J.P., and Langer, R. Progress in tissue engineering. Sci Am **300,** 64, 2009.
2. Ghaemmaghami, A.M., Hancock, M.J., Harrington, H., Kaji, H., and Khademhosseini, A. Biomimetic tissues on a chip for drug discovery. Drug Discov Today **17,** 173, 2012.
3. Anderson, R.H., Smerup, M., Sanchez-Quintana, D., Loukas, M., and Lunkenheimer, P.P. The three-dimensional arrangement of the myocytes in the ventricular walls. Clin Anat **22,** 64, 2009.
4. Fay, F.S., and Delise, C.M. Contraction of isolated smooth-muscle cells - structural changes. Proc Natl Acad Sci U S A **70,** 641, 1973.
5. Lieber, R.L., and Bodine-Fowler, S.C. Skeletal muscle mechanics: implications for rehabilitation. Phys Ther **73,** 844, 1993.
6. Khademhosseini, A., Langer, R., Borenstein, J., and Vacanti, J.P. Microscale technologies for tissue engineering and biology. Proc Natl Acad Sci U S A **103,** 2480, 2006.
7. Wigmore, P.M., and Dunglison, G.F. The generation of fiber diversity during myogenesis. Int J Dev Biol **42,** 117, 1998.
8. Slaughter, B.V., Khurshid, S.S., Fisher, O.Z., Khademhosseini, A., and Peppas, N.A. Hydrogels in regenerative medicine. Adv Mater **21,** 3307, 2009.
9. Annabi, N., Nichol, J.W., Zhong, X., Ji, C.D., Koshy, S., Khademhosseini, A., *et al.* Controlling the porosity and microarchitecture of hydrogels for tissue engineering. Tissue Eng Part B Rev **16,** 371, 2010.
10. Wheeldon, I., Ahari, A.F., and Khademhosseini, A. Microengineering hydrogels for stem cell bioengineering and tissue regeneration. JALA **15,** 440, 2010.
11. Du, Y.A., Ghodousi, M., Qi, H., Haas, N., Xiao, W.Q., and Khademhosseini, A. Sequential assembly of cell-laden hydrogel constructs to engineer vascular-like microchannels. Biotech Bioeng **108,** 1693, 2011.
12. Wheeldon, I., Farhadi, A., Bick, A.G., Jabbari, E., and Khademhosseini, A. Nanoscale tissue engineering: spatial control over cell-materials interactions. Nanotechnology **22,** 212001, 2011.
13. Nagamine, K., Kawashima, T., Ishibashi, T., Kaji, H., Kanzaki, M., and Nishizawa, M. Micropatterning contractile C2C12 myotubes embedded in a fibrin gel. Biotech Bioeng **105,** 1161, 2010.
14. Gupta, P., Vermani, K., and Garg, S. Hydrogels: from controlled release to pH-responsive drug delivery. Drug Discov Today **7,** 569, 2002.
15. Chen, C.S., Mrksich, M., Huang, S., Whitesides, G.M., and Ingber, D.E. Geometric control of cell life and death. Science **276,** 1425, 1997.
16. Jiang, X.Y., Takayama, S., Qian, X.P., Ostuni, E., Wu, H.K., Bowden, N., *et al.* Controlling mammalian cell spreading and cytoskeletal arrangement with conveniently fabricated continuous wavy features on poly(dimethylsiloxane). Langmuir **18,** 3273, 2002.
17. Lin, C., and Bissell, M. Multi-faceted regulation of cell differentiation by extracellular matrix. FASEB J **7,** 737, 1993.
18. Krauss, R.S., Cole, F., Gaio, U., Takaesu, G., Zhang, W., and Kang, J-S. Close encounters: regulation of vertebrate skeletal myogenesis by cell-cell contact. J Cell Sci **118,** 2355, 2005.
19. Nichol, J.W., Koshy, S.T., Bae, H., Hwang, C.M., Yamanlar, S., and Khademhosseini, A. Cell-laden microengineered gelatin methacrylate hydrogels. Biomaterials **31,** 5536, 2010.
20. Khademhosseini, A., and Langer, R. Microengineered hydrogels for tissue engineering. Biomaterials **28,** 5087, 2007.
21. Boontheekul, T., Hill, E.E., Kong, H-J., and Mooney, D.J. Regulating myoblast phenotype through controlled gel stiffness and degradation. Tissue Eng **13,** 1431, 2007.

22. Engler, A.J., Griffin, M.A., Sen, S., Bönnemann, C.G., Sweeney, H.L., and Discher, D.E. Myotubes differentiate optimally on substrates with tissue-like stiffness. J Cell Biol **166,** 877, 2004.
23. Lam, M.T., Huang, Y.C., Birla, R.K., and Takayama, S. Microfeature guided skeletal muscle tissue engineering for highly organized 3-dimensional free-standing constructs. Biomaterials **30,** 1150, 2009.
24. Clark, P., Dunn, G.A., Knibbs, A., and Peckham, M. Alignment of myoblasts on ultrafine gratings inhibits fusion *in vitro*. Int J Biochem Cell Biol **34,** 816, 2002.
25. Charest, J.L., Eliason, M.T., Garcia, A.J., and King, W.P. Combined microscale mechanical topography and chemical patterns on polymer cell culture substrates. Biomaterials **27,** 2487, 2006.
26. Glawe, J.D., Hill, J.B., Mills, D.K., and McShane, M.J. Influence of channel width on alignment of smooth muscle cells by high-aspect-ratio microfabricated elastomeric cell culture scaffolds. J Biomed Mat Res Part A **75,** 106, 2005.
27. Vader, D., Kabla, A., Weitz, D., and Mahadevan, L. Strain-induced alignment in collagen gels. PLOS One **4,** e5902, 2009.
28. Nguyen, T.D., Liang, R., Woo, S.L.Y., Burton, S.D., Wu, C.F., Almarza, A., *et al.* Effects of cell seeding and cyclic stretch on the fiber remodeling in an extracellular matrix-derived bioscaffold. Tissue Eng Part A **15,** 957, 2009.
29. Flaibani, M., Boldrin, L., Cimetta, E., Piccoli, M., De Coppi, P., and Elvassore, N. Muscle differentiation and myotubes alignment is influenced by micropatterned surfaces and exogenous electrical stimulation. Tissue Eng Part A **15,** 2447, 2009.
30. Powell, C.A., Smiley, B.L., Mills, J., and Vandenburgh, H.H. Mechanical stimulation improves tissue-engineered human skeletal muscle. Am J Physiol Cell Physiol **283,** C1557, 2002.
31. Bursac, N., Bian, W.N., Liau, B., and Badie, N. Mesoscopic hydrogel molding to control the 3D geometry of bioartificial muscle tissues. Nat Protoc **4,** 1522, 2009.
32. Aubin, H., Nichol, J.W., Hutson, C.B., Bae, H., Sieminski, A.L., Cropek, D.M., *et al.* Directed 3D cell alignment and elongation in microengineered hydrogels. Biomaterials **31,** 6941, 2010.
33. Peckham, P.H., Mortimer, J.T., and Marsolais, E.B. Alteration in the force and fatigability of skeletal muscle in quadriplegic humans following exercise induced by chronic electrical stimulation. Clin Orthop Relat Res **114,** 326, 1976.
34. Dhawan, V., Lytle, I.F., Dow, D.E., Huang, Y.C., and Brown, D.L. Neurotization improves contractile forces of tissue-engineered skeletal muscle. Tissue Eng **13,** 2813, 2007.
35. Ostrovidov, S., Jiang, J., Sakai, Y., and Fujii, T. Membrane-based PDMS microbioreactor for perfused 3D primary rat hepatocyte cultures. Biomed Microdevices **6,** 279, 2004.
36. Nelson, C.M., Inman, J.L., and Bissell, M.J. Three-dimensional lithographically defined organotypic tissue arrays for quantitative analysis of morphogenesis and neoplastic progression. Nat Protoc **3,** 674, 2008.
37. Ren, K., Crouzier, T., Roy, C., and Picart, C. Polyelectrolyte multilayer films of controlled stiffness modulate myoblast cell differentiation. Adv Funct Mater **18,** 1378, 2008.
38. Kaji, H., Ishibashi, T., Nagamine, K., Kanzaki, M., and Nishizawa, M. Electrically induced contraction of C2C12 myotubes cultured on a porous membrane-based substrate with muscle tissue-like stiffness. Biomaterials **31,** 6981, 2010.
39. Discher, D.E., Janmey, P., and Wang, Y-l. Tissue cells feel and respond to the stiffness of their substrate. Science **310,** 1139, 2005.
40. King, W.P., Charest, J.L., and Garcia, A.J. Myoblast alignment and differentiation on cell culture substrates with microscale topography and model chemistries. Biomaterials **28,** 2202, 2007.
41. Bischofs, I.B., and Schwarz, U.S. Cell organization in soft media due to active mechanosensing. Proc Natl Acad Sci U S A **100,** 9274, 2003.
42. Clark, P., Connolly, P., Curtis, A.S., Dow, J.A., and Wilkinson, C.D. Cell guidance by ultrafine topography *in vitro*. J Cell Sci **99,** 73, 1991.
43. Bajaj, P., Reddy, B., Millet, L., Wei, C., Zorlutuna, P., Bao, G., *et al.* Patterning the differentiation of C2C12 skeletal myoblasts. Integr Biol **3,** 897, 2011.
44. Yamasaki, K-I., Hayashi, H., Nishiyama, K., Kobayashi, H., Uto, S., Kondo, H., *et al.* Control of myotube contraction using electrical pulse stimulation for bio-actuator. J Artif Organs **12,** 131, 2009.
45. Pedrotty, D.M., Koh, J., Davis, B.H., Taylor, D.A., Wolf, P., and Niklason, L.E. Engineering skeletal myoblasts: roles of three-dimensional culture and electrical stimulation. Am J Physiol Heart Circ Physiol **288,** H1620, 2005.
46. Tandon, N., Marsano, A., Maidhof, R., Numata, K., Montouri-Sorrentino, C., Cannizzaro, C., Voldmand, J., and Vunjak-Novakovic, G. Surface-patterned electrode bioreactor for electrical stimulation. Lab Chip **10,** 692, 2010.
47. Tandon, N., Cannizzaro, C., Chao, P-H.G., Maidhof, R., Marsano, A., Au, H.T.H., Radisic, M., and Vunjak-Novakovic, G. Electrical stimulation systems for cardiac tissue engineering. Nat Protoc **4,** 155, 2009.
48. Au, H.T.H., Cheng, I., Chowdhury, M.F., and Radisic, M. Interactive effects of surface topography and pulsatile electrical field stimulation on orientation and elongation of fibroblasts and cardiomyocytes. Biomaterials **28,** 4277, 2007.
49. Au, H.T.H., Cui, B.O., Chu, Z.E., Veres, T., and Radisic, M. Cell culture chips for simultaneous application of topographical and electrical cues enhance phenotype of cardiomyocytes. Lab Chip **9,** 564, 2009.
50. Bhana, B., Iyer, R.K., Chen, W.L.K., Zhao, R., Sider, K.L., Likhitpanichkul, M., Simmons, C.A., and Radisic, M. Influence of substrate stiffness on the phenotype of heart cells. Biotechnol Bioeng **105,** 1148, 2010.
51. Liao, I.C., Liu, J., Bursac, N., and Leong, K. Effect of electromechanical stimulation on the maturation of myotubes on aligned electrospun fibers. Cell Mol Bioeng **1,** 133, 2008.
52. Folland, J.P., and Williams, A.G. The adaptations to strength training: morphological and neurological contributions to increased strength. Sports Med **37,** 145, 2007.

Address correspondence to:
Ali Khademhosseini, Ph.D.
Department of Medicine
Center for Biomedical Engineering
Brigham and Women's Hospital
Harvard Medical School
65 Landsdowne St.
Cambridge, MA 02139

E-mail: alik@rics.bwh.harvard.edu

Received: March 21, 2012
Accepted: June 13, 2012
Online Publication Date: October 24, 2012